Supporting Information

Active oxygen species on Mg-La mixed oxides: the effect of Mg and La oxide interactions

Xianyuan Wu,[a] Zheng Fang,[a] Hui Pan,[b] Yifan Zheng,[a] Dahao Jiang,[a] Jun Ni*[a] and Xiaonian Li*[a]

[a]*Institute of Industrial Catalysis, College of Chemical Engineering, Zhejiang University of Technology, Hangzhou, 310014, China.*

[b]*Institute of Applied Physics and Materials Engineering, University of Macau, China*

Corresponding author. Tel.: (+86)571 8832 0092; E-mail address: Junni@zjut.edu.cn (J. N.)

This file includes:

Experimental Methods

Figs. S1 to S11

Tables S1 and S2

Experimental methods

Catalyst synthesis

Different particle sized Mg-La mixed oxide catalysts were prepared using modified reverse microemulsion systems [*J. Mater. Chem.*, 2007, **17**, 2257-2266], with the molar ratio of water to surfactant ω = 20, 30, 40 and 50, respectively. Typically, 300.00 g $Mg(NO_3)_2 \cdot 6H_2O$ (Aladdin, 99.0%) and 50.66 g $La(NO_3)_3 \cdot 6H_2O$ (Aladdin, 99.0%) were dissolved in 401 ml de-ionized water in 500 ml conical flask to make **Solution A**. 80.00g NaOH (Aladdin, 99.99%) were dissolved in 500 ml de-ionized water in 500 ml volumetric flask to make **Solution B**. To prepare the catalyst with ω = 50, 48.0 ml **Solution A** was added dropwisely into 1661.6 ml isooctane containing 23.93 g sodium dodecylsulfate (SDS) and 25.26 g 1-butanol in a 2 L three-neck round-bottom flask to make a clear system at temperature of 60 ºC. 156 ml of **Solution B** was then added dropwisely into the former system afterwards. The mixture turned from slightly translucent to milky solids and was further heated at 60 ºC for 6 h. All the above mentioned mixing and reaction processes were carried out with continuous mechanical stirring at 500 rpm. The gel-like solids were separated by centrifugation at 11000 rpm. In order to remove all the nitrate salts and unreacted SDS, the solids were refluxed in an ethanol–water (1 : 1 in volume) mixture (total volume 1000 mL) for 4 h before centrifugation. This procedure was repeated ten times. The solid finally obtained was dried in air at temperature of 80 ºC and hand-ground in an agate mortar to yield a fine powder. It was stored in a desicator with anhydrous $CaCl_2$. Prior to catalyst characterizations and activity tests, the solid was calcined in air at 800 ºC for 1h. The prepared catalysts were designated as Mg-La-20, Mg-La-30, Mg-La-40, and Mg-La-50, respectively, in which the number stands for the ω value.

Catalyst characterizations

1. N_2 adsorption-desorption

The BET specific surface area of calcined catalysts was measured from the N_2 adsorption and desorption isotherms collected on Quantachrome Autosorb-6 at 77 K. Prior to the measurement, all samples were degassed at 300 °C until a stable vacuum of approximately 5 mTorr was reached.

2. Powder X-ray diffraction (XRD)

XRD patterns were collected with a Bruker D8 Advance X-ray diffraction system equipped with $Cu_{K\alpha}$ radiation ($\lambda = 0.154$ nm), at a step width of 0.02° in the (2θ) range from 20° to 90°. Structure refinement was carried out via the Rietveld method with the JADE 9.0 software until the weighted residual was minimized.

3. High resolution transmission electron microscopy (HRTEM)

HRTEM images of Mg-La mixed oxides were acquired in Fei Tecnai G2 TF20 S-twin microscope. The samples were prepared by placing a drop of nanoparticle-ethanol suspension onto a carbon-coated copper grid, then allowing the solvent to evaporate.

4. Temperature Programmed Reduction (TPR)

H_2-TPR was performed on a home-made apparatus equipped with mass spectrometer (HIDEN ANALYTICAL QIC-20), as shown in Fig. S1. The catalysts of 200 mg, which had been thermally treated under Ar stream at 300 °C for 1 h to remove water and other contaminants, were heated from 30 °C to 800 °C at a rate of 10 °C /min in 50 ml/min of 5% of H_2/Ar and maintained at 800 °C for 10 min, while mass spectrometer signals at m/e of 44, 32, 28, 18, 16 and 2 were monitored.

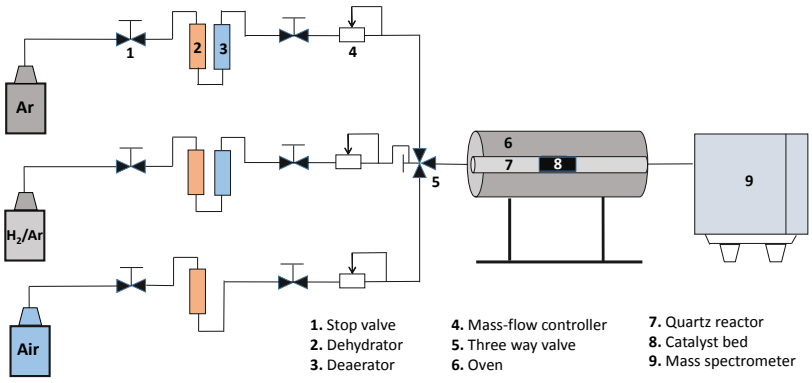

Fig. S1. The configuration of the apparatus used for H_2-TPR.

5. Temperature Programmed Desorption (TPD)

O_2-TPD was performed in the same apparatus as above for H_2-TPR. The catalysts of 200 mg, which had been thermally treated in air at 800 °C for 1 h, were heated from 30 °C to 800 °C at a rate of 5 °C /min in 30 ml/min of Ar, while mass spectrometer signals at m/e of 44, 32, 28, 18, 16 and 2 were

monitored.

6. X-ray photoelectron spectroscopy (XPS)

XPS data were obtained with an ESCALab220i-XL electron spectrometer from VG Scientific using 300W $Al_{K\alpha}$ radiation. The base pressure was about 3×10^{-9} mbar. The C 1s peak of adventitious carbon at 284.5 eV was used as a reference for energy corrections. All samples were calcined in a special designed system and transferred under Ar protection into the XPS chamber.

7. Temperature Programmed Surface Reaction (TPSR)

CH_4-TPSR of the catalysts was performed in the same apparatus as above for H_2-TPR. For each run, 200 mg of the catalyst was placed in the quartz tube. All the samples were first treated with a pure CO_2 flowing at 25 mL/min from ambient to 700°C with a temperature programmed ramping rate 10°C/min. This was followed by cooling down to 120 °C in CO_2 and then Ar flushing at 30 mL/min for 60 min. After this step, a mixture of 10% CH_4/Ar flowing at 30 ml/min was introduced while the temperature of catalyst bed was increased linearly from 120 to 800 °C at 10 °C/min. Reaction products signals at m/e of 44, 28, 18, 16 and 2 were continuously recorded by the mass spectrometer. The product CO signals were used to monitor the reaction between CH_4 and $La_2O_2CO_3$. The CO signals were corrected for contribution of CO_2 cracking in the mass spectrometer because the cracking of CO_2 in the MS significantly contributed to the CO MS signals.

8. First-principles calculations

First-principles calculations to investigate the interaction between MgO and La_2O_3 on the basis of the density functional theory (DFT) [*Phys. Rev.*, 1964, 136, B864-B871] and the Perdew-Burke-Eznerhof generalized gradient approximation (PBE-GGA) [*Phys. Rev. B*, 1994, 50, 17953-17979]. The Vienna ab initio simulation package (VASP) [*Phys. Rev. Lett.*, 1996, 77, 3865-3868] incorporated with projector augmented wave (PAW) scheme [*Phys. Rev. B*, 1999, 59, 1758-1775; *Phys. Rev. B*, 1996, 54, 11169-11186] is used to perform the calculations. K point sampling for integration over the first Brillouin zone is based on the Monkhorst and Pack scheme [*Phys. Rev. B*, 1976, 13, 5188-5192]. A 5×5×5 grid for k-point sampling for geometry optimization and calculations of density of states, respectively, and an energy cut-off of 500 eV are consistently used

in our calculations. Good convergence is obtained with these parameters and the total energy was converged to 2.0×10^{-5} eV/atom.

9. Oxidative Coupling of Methane (OCM) activity

The OCM activity was evaluated in a fixed bed quartz tubular reactor with an inner diameter of 8 mm and an online gas chromatograph (GC) for product monitoring equipped with two detectors, a thermal conductivity detector (TCD) and a flame ionization detector (FID). For loading the reactor, 100 mg of catalyst was supported in the quartz reactor tube between two pieces of quartz wool. The catalyst was pretreated in air with 30 ml/min flow rate at 800 °C for 1 h. When the catalyst temperature decreased to 400 °C, the reactant gases (CH_4 and O_2) and an internal standard N_2 were fed into the fixed bed reactor at a total rate of 30 ml/min which consist of 20 ml/min methane and 5 ml/min oxygen. The CH_4/O_2 feed ratio was held constant at 4:1 for all experiments because this is the stoichiometric amount needed for conversion of methane to ethane and water. A cold trap was placed at the outlet of the quartz reactor to separate any condensed water vapor from the reaction products. The activity and selectivity of catalysts were measured as a function of temperature by increasing the temperature in 100 °C intervals until the temperature reached 800 °C. The methane conversion (X_{CH_4}) is calculated by the difference of the methane entering the reactor system and the unconverted methane in the reactor effluent as determined by the GC (eq 1). The C_2 selectivity (S_{C_2}, eq 2) is the fraction of methane converted to C_2 products in the total amount of methane converted to CO, CO_2, and C_2 plus C_3 products. The C_2 yield (Y_{C_2}), is calculated by multiplying the methane conversion (X_{CH_4}) and the C_2 selectivity (S_{C_2}) as described in eq 3.

$$X_{CH_4} = \frac{CH_{4,\,in} - CH_{4,\,out}}{CH_{4,\,in}} \quad (1)$$

$$S_{C_2} = \frac{mole\ of\ CH_4\ reacted\ to\ C_2\ products}{mole\ of\ CH_4\ reacted\ to\ CO_x, C_2,\ and\ C_3\ products} \quad (2)$$

$$Y_{C_2} = X_{CH_4} \cdot S_{C_2} \quad (3)$$

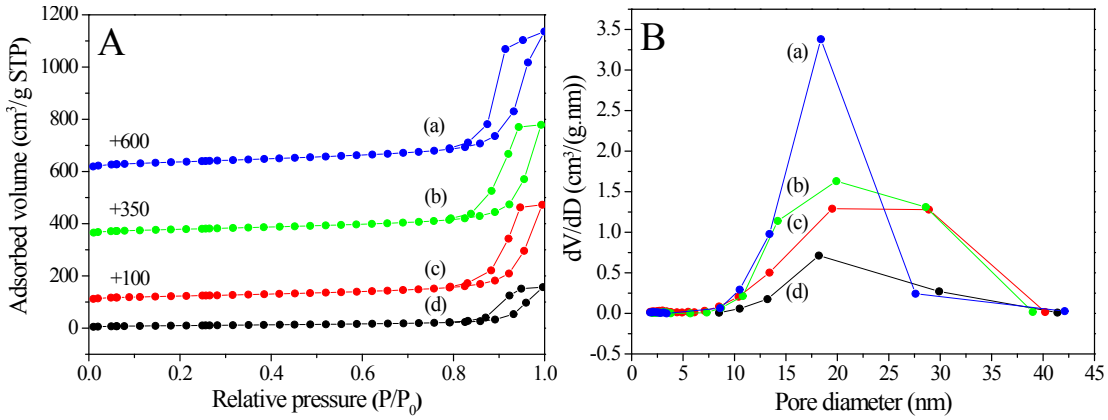

Fig. S2 Nitrogen adsorption–desorption isotherms (A) and pore diameter distributions (B) of the catalysts: (a) Mg-La-20; (b) Mg-La-30; (c) Mg-La-40; (d) Mg-La-50.

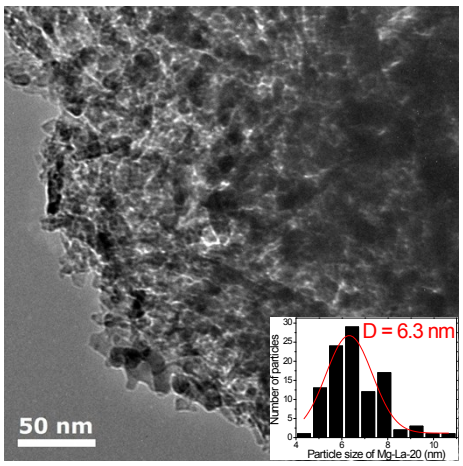

Fig. S3 TEM image of Mg-La-20 catalyst and particle size distribution.

As shown in Fig. S3, the average particle size for the Mg-La-20 catalyst calculated over 100 particles in the TEM image is 6.3 nm.

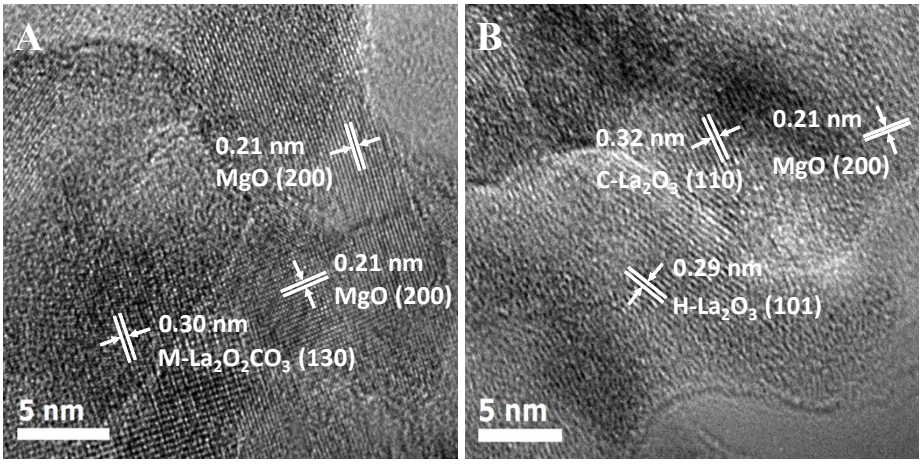

Fig. S4 HRTEM images of Mg-La-20 catalyst.

The presence of M-$La_2O_2CO_3$ over Mg-La-20 catalyst is shown in Fig. S4A. The close contact of M-$La_2O_2CO_3$ with MgO, which is the same case between C-La_2O_3 and MgO, indicates the formation of M-$La_2O_2CO_3$ is derived from the reaction of C-La_2O_3 with CO_2. In contrast, when La_2O_3 is far away from MgO, only H-La_2O_3 is observed (Fig. S4B). This further emphasizes the importance of intimate interaction between La_2O_3 and MgO.

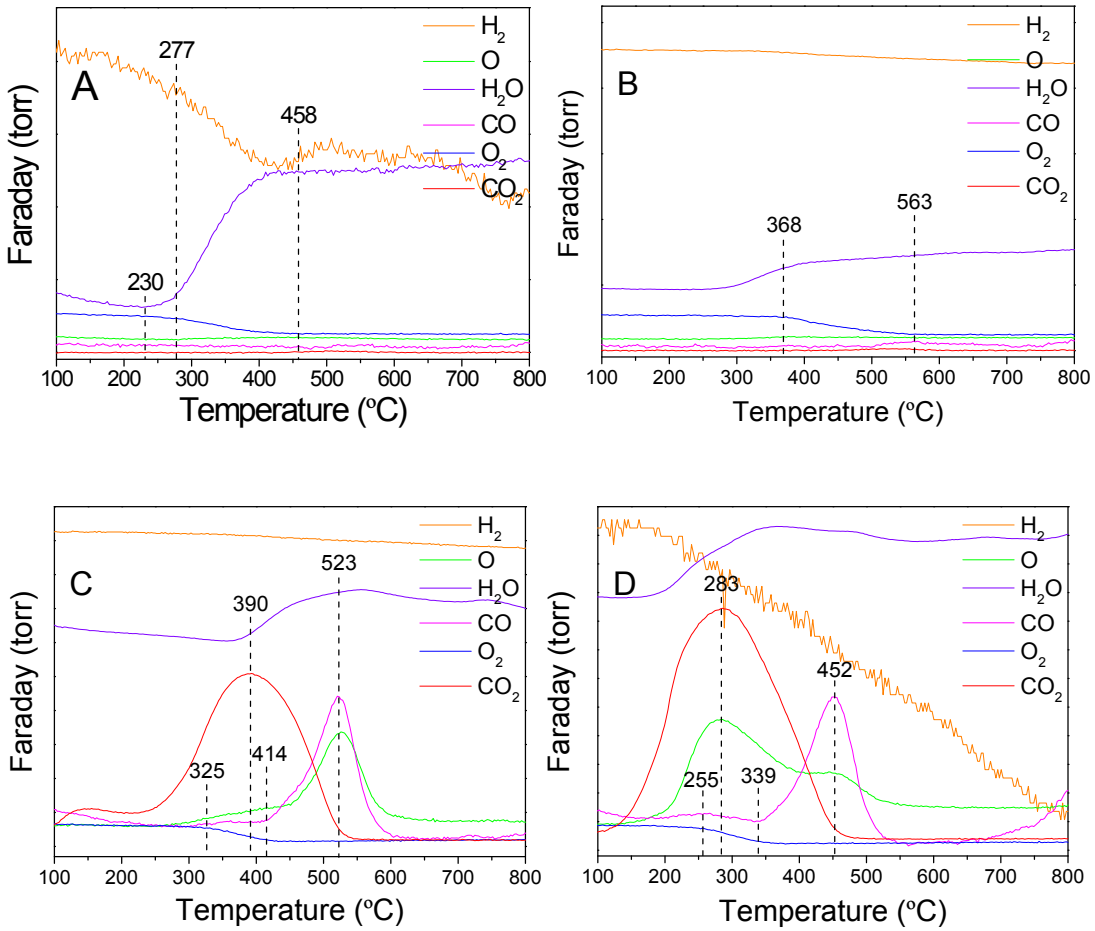

Fig. S5 H_2-TPR profiles of calcined catalysts: A. Mg-La-50; B. Mg-La-40; C. Mg-La-30; D. Mg-La-20.

The O_2 signals corresponded to the consumption of oxygen remained in the H_2-TPR apparatus. In the course of H_2-TPR, the surface adsorbed oxygen species on Mg-La-ω oxides was firstly reduced and then supplemented by the oxygen via a Mars-van Krevelen mechanism at temperatures lower than 400 °C. The CO and O signals were the result of the reaction of M-$La_2O_2CO_3$ with H_2, generating CO, La_2O_3 and H_2O. And then H_2O split into H and O in mass spectroscopy. The desorbed CO_2 signals were ascribed to the decomposition of M-$La_2O_2CO_3$ in H_2 at lower temperatures, while at higher temperatures M-$La_2O_2CO_3$ reacted with H_2.

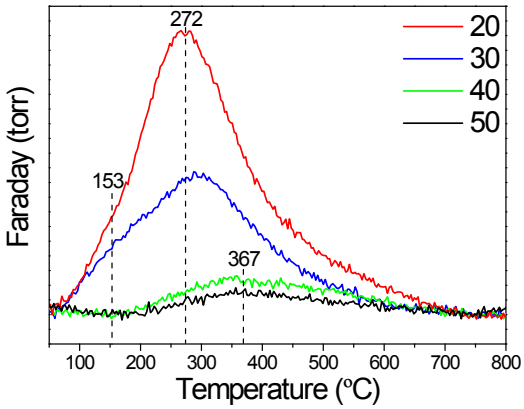

Fig. S6 O_2-TPD profiles of Mg-La mixed oxide catalysts

O_2-TPD profiles show the feature of the adsorbed oxygen from Mg-La mixed oxide catalysts. O_2-TPD was performed with a flow of 30 ml/min Ar and a heating rate of 5 °C /min to 800 °C. Three distinct desorption peaks of oxygen from the Mg-La-20 catalyst are observed: a shoulder peak at 153 °C should be attributed to the desorption of adsorbed molecular species, a strong symmetric peak and another shoulder peak at 272 and 367 °C can be correlated to the desorption of adsorbed surface oxygen species O_2^- and O^-, respectively [*Catal. Today*, 1990, 6, 473; *Nanoscale*, 2013, 5, 10844-10848]. There is only a faint broad peak centered at 367 °C detected on the Mg-La-40 and Mg-La-50 catalysts, indicating much less amount of oxygen species than Mg-La-30 and Mg-La-20 catalysts.

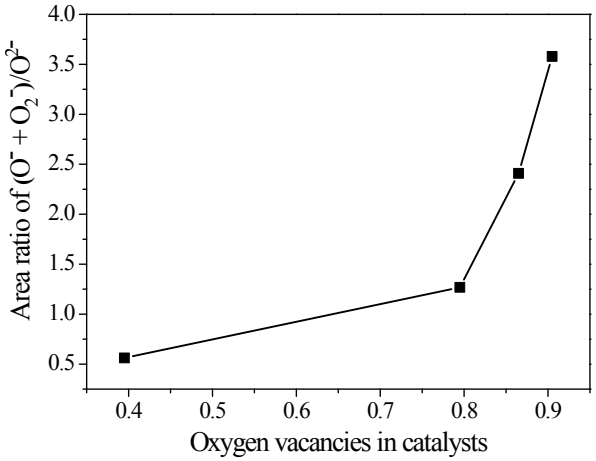

Fig. S7 Correlation between the oxygen vacancies with the relative contents of surface adsorbed oxygen species.

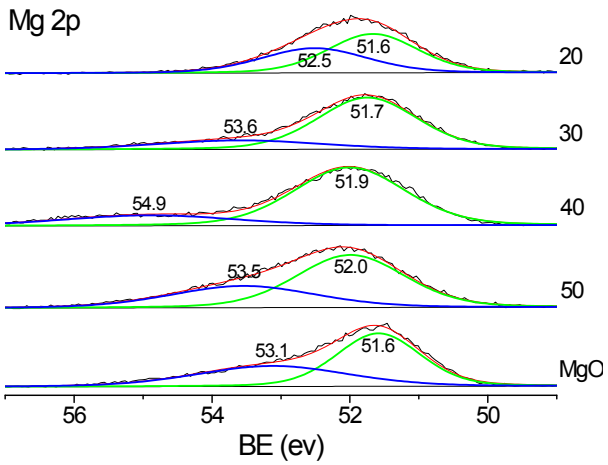

Fig. S8 O1s binding energy spectra of Mg-La mixed oxide catalysts and MgO.

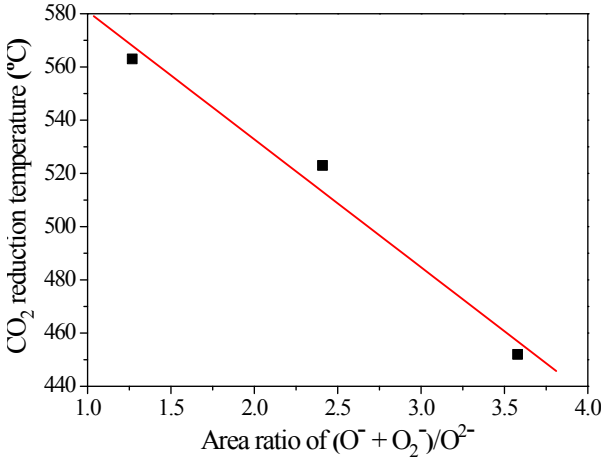

Fig. S9 Correlation between the relative contents of surface adsorbed oxygen species with CO_2 reduction temperatures.

Table S1 Lattice parameters for pure oxides and doped oxides

	MgO	C-La_2O_3	La-doped MgO	H-La_2O_3	Mg-doped H-La_2O_3
Lattice Constant (nm)	a = 0.4245	a = 1.1397	a = 0.4530	a = 0.3939 c = 0.6136	a = 0.38807 c = 0.62569

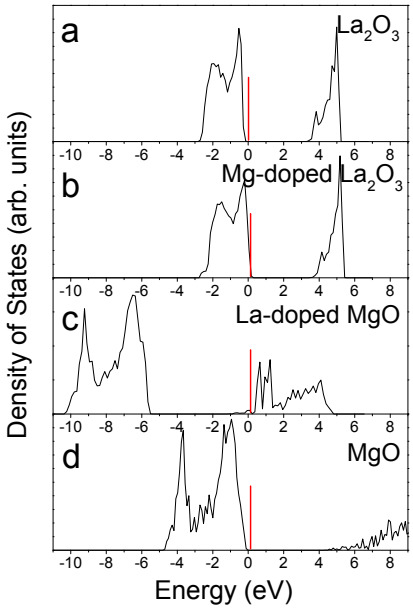

Fig. S10 Densities of states for cubic La_2O_3, Mg doped La_2O_3, La doped MgO and MgO.

First-principles calculations were utilized to investigate the interaction between MgO and La_2O_3 on the basis of the density functional theory (DFT) and the Perdew-Burke-Eznerhof generalized gradient approximation (PBE-GGA). Because it is very difficult to build a model for Mg-La mixed oxides, instead we investigated the cases where MgO was doped with La and La_2O_3 was doped with Mg. As shown in Table S1, the lattice parameters are obtained by relaxing MgO and cubic La_2O_3 unit cell. A 2×2×2 supercell of MgO is used to investigate the effect of La incorporation on its lattice constant. The calculated lattice constants show that La-doping leads to the expansion of the lattice of MgO by 6.7% at a doping concentration of 12.5%. Similarly, Mg-doping also results in the expansion of the lattice of H-La_2O_3 by 1.97% at a doping concentration of 12.5%. The calculated total density of states (TDOSs) shows that La_2O_3 (Fig. S10a) and MgO (Fig. S10d) are insulators/semiconductors with band gap larger than 3.5 eV. The doping of La into MgO introduces electrons into MgO, as indicated by the Fermi level (red line at 0 eV) in the bottom conduction band (Fig. S10c), while the doping of Mg into La_2O_3 introduces vacancies into La_2O_3, as indicated by the Fermi level in the valence band (Fig. S10b). Both results suggest the charge transfer from La_2O_3 to MgO in the heterojuntions. Combining the results from Rietveld refinements of the XRD patterns (Table S2), we realized that it is the doping of Mg into cubic La_2O_3, which introduces vacancies into La_2O_3, facilitates the charge transfer from La_2O_3 to MgO.

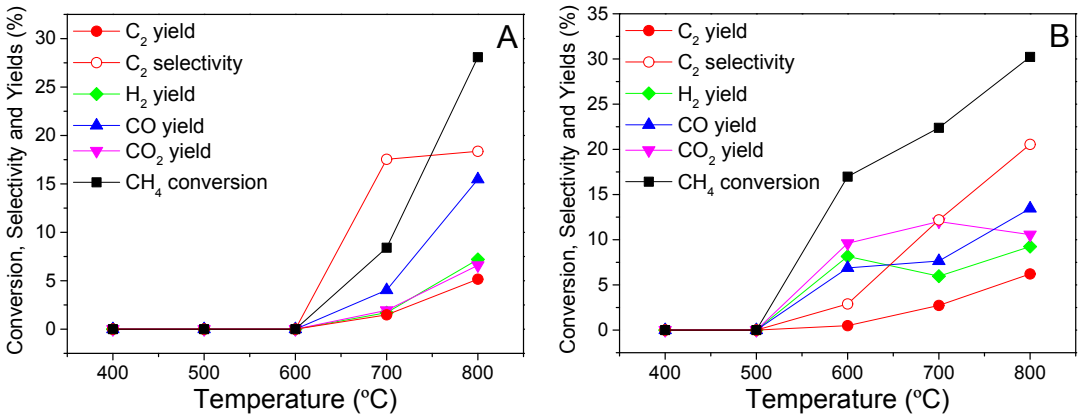

Fig. S11 Reaction data during oxidative coupling of methane as a function of temperature obtained over (A) MgO and (B) Mg-La-20 catalysts at a CH_4/O_2 ratio of 4:1.

The oxidative coupling of methane (OCM) activity was evaluated in a fixed bed quartz tubular reactor with at a CH_4/O_2 ratio of 4:1 (20 ml/min methane and 5 ml/min oxygen) at atmospheric pressure. MgO has been used as a reference catalyst for the comparison with Mg-La-20 catalyst. The methane conversion, ethane and ethylene (C_2) selectivity and yield, and the yields for H_2, CO and CO_2 are displayed in Fig. S11. The Mg-La-20 catalyst has a lower onset temperature for OCM reaction than MgO, and superior performance in both methane conversion and C_2 yield. Apart from C_2 products, the Mg-La-20 catalyst also produces higher amounts of CO and CO_2, indicating that the Mg-La-20 catalyst has higher amounts of surface adsorbed oxygen species for oxidation reactions.

Table S2 Phase composition, mass fraction and unit cell parameters of Mg-La mixed oxide catalysts.

Catalyst	Phase composition	Mass fraction (%)	Unit cell parameters (nm)		
			a	*b*	*c*
Mg-La-20	Cubic MgO	50.4	0.42126	0.42126	0.42126
	Hexagonal La_2O_3	3.6	0.392809	0.392809	0.613349
	Cubic La_2O_3	28.2	1.160569	1.160569	1.160569
	Monoclinic La_2O_3	17.8	1.576812	0.386539	0.876135
Mg-La-30	Cubic MgO	66.6	0.422437	0.422437	0.422437
	Hexagonal La_2O_3	6.9	0.394856	0.394856	0.616316
	Cubic La_2O_3	21.4	1.169661	1.169661	1.169661
	Monoclinic La_2O_3	5.1	1.591324	0.388081	0.881544
Mg-La-40	Cubic MgO	55.5	0.421584	0.421584	0.421584
	Hexagonal La_2O_3	14.2	0.393591	0.393591	0.614109
	Cubic La_2O_3	17.0	1.146691	1.146691	1.146691
	Monoclinic La_2O_3	13.4	1.567144	0.389286	0.876907
Mg-La-50	Cubic MgO	52.6	0.421732	0.421732	0.421732
	Hexagonal La_2O_3	17.5	0.393949	0.393949	0.614565
	Cubic La_2O_3	12.7	1.134347	1.134347	1.134347
	Monoclinic La_2O_3	17.2	1.575348	0.390484	0.876243
Cubic MgO: Fm-3m (225), Z=4, cF8 [PDF#98-000-0349]; Hexagonal La_2O_3: P-3m1 (164), Z=1, hP5 [PDF#04-005-5955]; Cubic La_2O_3: Ia-3 (206), Z=16, cI80 [PDF#00-022-0369]; Monoclinic La_2O_3: C2/m (12) <b-unique>, Z=6, mC30 [PDF#04-002-3877].					

The structure refinement results show that with the decrease in ω value, the mass fraction of hexagonal La_2O_3 decreases from 17.5 wt% for Mg-La-50 to 3.6 wt% for Mg-La-20, whereas the mass fraction of cubic La_2O_3 increases from 12.7 wt% for Mg-La-50 to 28.2 wt% for Mg-La-20. Meanwhile the mass fraction of monoclinic La_2O_3 varies relatively insignificantly, the presence of which has been recognized as active sites for the combustion of propene at 673 K [*Chem. Lett.*, 1986, 1333-1336]. The formation of monoclinic La_2O_3 is supposed to be the result of strong interaction of MgO with La_2O_3, although the reason for its formation is not certain.

Comparing with the lattice constant of MgO (0.4245 nm), all the lattice constants of MgO in Mg-La mixed oxides reduce to different extents. Smaller lattice constant of MgO can be obtained when decreasing the ω value. On the other hand, the lattice constant of cubic La_2O_3 increases from 1.13270 nm for pure cubic La_2O_3 and 1.134347 nm for Mg-La-50 to 1.160569 nm for Mg-La-20. Approximately 2.31% expansion of the cubic La_2O_3 lattice is observed. Our theoretical calculations (Table S1 and Fig. S10) have revealed the La-doping into MgO leads to the expansion of MgO lattice by 6.7% at a doping concentration of 12.5%. Similarly, Mg-doping into H-La_2O_3 also results in the expansion of H-La_2O_3 lattice by 1.97% at a doping concentration of 12.5%. Thus, the contraction of MgO lattice and the expansion of cubic La_2O_3 lattice both indicate that there is a Mg-doping into cubic La_2O_3 over Mg-La mixed oxides. The intimate contact between MgO and La_2O_3 is favorable for this doping, and benefits the formation of vacancies in La_2O_3, as a result of which also the charge transfer from La_2O_3 to MgO in the heterojuntions.